Opto-Electronic Advances

Review

2021, Vol. 4, No. 11

DOI: 10.29026/oea.2021.210030

Recent advances in optical dynamic meta-holography

Hui Gao[1†], Xuhao Fan[1†], Wei Xiong[1*] and Minghui Hong[2]

Holography, with the capability of recording and reconstructing wavefronts of light, has emerged as an ideal approach for future deep-immersive naked-eye display. However, the shortcomings (e.g., small field of view, twin imaging, multiple orders of diffraction) of traditional dynamic holographic devices bring many challenges to their practical applications. Metasurfaces, planar artificial materials composed of subwavelength unit cells, have shown great potential in light field manipulation, which is useful for overcoming these drawbacks. Here, we review recent progress in the field of dynamic metasurface holography, from realization methods to design strategies, mainly including typical research works on dynamic meta-holography based on tunable metasurfaces and multiplexed metasurfaces. Emerging applications of dynamic meta-holography have been found in 3D display, optical storage, optical encryption, and optical information processing, which may accelerate the development of light field manipulation and micro/nanofabrication with higher dimensions. A number of potential applications and possible development paths are also discussed at the end.

Keywords: metasurface; dynamic meta-holography; tunable meta-holography; multiplexed meta-holography

Gao H, Fan XH, Xiong W, Hong MH. Recent advances in optical dynamic meta-holography. *Opto-Electron Adv* **4**, 210030 (2021).

Introduction

In science fiction movies (e.g., Star Wars), naked-eye three-dimensional (3D) display scenes are so fantastic that they have attracted much attention to develop related technologies. Via recording and reconstructing wavefronts of light, holography is an ideal technology to achieve naked-eye 3D display as well as many optical applications, including optical storage[1,2], optical encryption[3], optical information processing[4] and optical manipulation[5,6]. Holography technology would provide a wonderful naked-eye display platform to greatly enhance visual immersion and reality, change the methods of human-computer interaction and human-human communication, and revolutionize our daily lives. Traditional optical holography requires a complicated shooting process to record the interference pattern of light beams from target objects and a reference path[7]. Therefore, traditional optical holography cannot create a holographic reconstruction of a virtual object. In 1966, computer-generated holography (CGH) was invented by Brown and Lohman to overcome this limitation, in which interference patterns are generated by using physical optics theories[8]. Moreover, CGH can also provide dynamic holographic display by using digital light field modulators, such as spatial light modulators (SLMs) and digital micromirror devices (DMDs)[9,10]. However, there are many shortcomings resulting from the large pixel sizes and limited modulation principle that hinder further

[1]Wuhan National Laboratory for Optoelectronics, School of Optical and Electronic Information, Huazhong University of Science and Technology, Wuhan 430074, China; [2]Department of Electrical and Computer Engineering, National University of Singapore, Engineering Drive 3, Singapore 117576, Singapore.

[†]These authors contributed equally to this work.

[*]Correspondence: W Xiong, E-mail: weixiong@hust.edu.cn

Received: 3 March 2021; Accepted: 27 April 2021; Published online: 25 July 2021

development of holographic technology, such as the small field of view (FOV), twin imaging, narrow bandwidth and multiple orders of diffraction[11,12].

In recent years, with the enormous development of nanofabrication technologies, metasurfaces consisting of subwavelength nanostructures have attracted much attention in many optical research fields due to their powerful capabilities in modulating the amplitude, phase, and polarization[13,14] of light[15], such as beam splitters[16,17], metalenses[18–24], orbital angular momentum (OAM) devices[25–30] and structural color elements[31–35]. Holograms require complicated light field modulation capabilities, and therefore, metasurfaces can be utilized to achieve holographic display. The target CGH patterns for holographic reconstructions can be calculated by physical and mathematical theories, and various nanostructure arrays are arranged according to the designed distribution to compose target CGH patterns. Metasurfaces possess more powerful light modulation abilities that provide much more degrees of freedom to design holograms than conventional CGH devices. In addition, meta-holography has several advantages compared with conventional CGH, such as a higher spatial resolution, lower noise, a larger working frequency bandwidth and elimination of undesired diffraction orders[11,12,36]. Meta-holography can be divided into different types based on different classification methods. For example, there are three types of meta-holography according to the principle of the light field modulation component, including phase-only holography[37–41], amplitude-only holography[42–44] and complex amplitude holography[45–48] (typical works shown in Fig. 1). Additionally, meta-holography can be classified into the two categories of static meta-holography and dynamic meta-holography based on the number of optical images reconstructed from a single piece of a metasurface element. Static meta-holography means that only one fixed image can be reconstructed by meta-hologram elements, while dynamic meta-hologram elements can reconstruct more than one image. Dynamic meta-holography is more suitable for optical display and information processing applications than static meta-holography. For example, to achieve fantastic naked-eye 3D display scenes as shown in science fiction movies or to realize optical camouflage in military reconnaissance, dynamic display is a fundamental and essential capability.

There have been some excellent reviews about

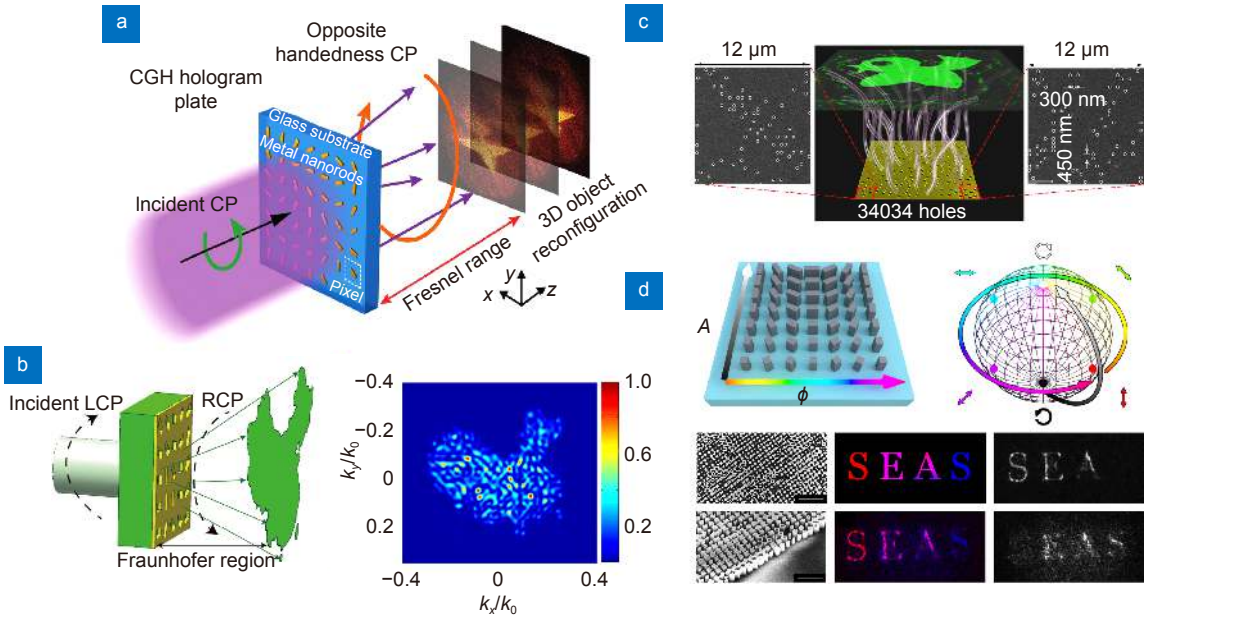

Fig. 1 | Typical examples of phase-only meta-holography, amplitude-only meta-holography and complex amplitude meta-holography. (**a**) 3D on-axis transmission-type phase-only meta-hologram composed of gold nanorod arrays[38]. (**b**) Phase-only metasurface-based broadband hologram with high tolerance to fabrication errors consisting of an elongated nanoaperture array[40]. (**c**) Amplitude-only meta-hologram enabled by a random photon sieve[42]. (**d**) Dielectric metasurface for complete and independent control of the optical amplitude and phase by adjusting the geometrical parameters and orientation angles of meta-atoms. The middle images are scanning electron microscopy (SEM) images of fabricated samples. Experimental reconstruction overlaying the separately measured pictures at 1.65 μm (marked as red color) and 0.94 μm (marked as blue color) wavelengths[48]. Figure reproduced with permission from: (a) ref.[38], under a Creative Commons Attribution 3.0 Unported Licence; (b) ref.[40], (d) ref.[48], under a Creative Commons Attribution 4.0 International License; (c) ref.[42], Springer Nature.

meta-holograms[49–51], which provided big pictures for this research field. Here we focused on the topic of dynamic meta-holography to give a comprehensive review for introducing recent development in this paper. Based on the realization methods, dynamic meta-holography can be mainly divided into two categories: tunable metasurfaces and multiplexed metasurfaces. We investigate these strategies and introduce typical research works on them. Furthermore, we also propose potential applications and possible development paths of dynamic meta-holography in the future.

Tunable meta-holography

The majority of metasurfaces are static and cannot be tuned after being fabricated. However, since the desire for plenty applications requiring active controlling, there are much effort devoted to exploit active materials and tuning methods[52,53], such as thermo-optic effects (e.g. silicon[54–56], lead telluride[57]), free -carrier effects (e.g. silicon[58–60], gallium arsenide[61–63], indium antimonide[64], indium tin oxide[65–68], graphene[69–71]), phase transitions (e.g. liquid crystals[72,73], germanium–antimony–tellurium (GST)[74–80], vanadium dioxide (VO_2)[81–84]), stretchable structures[85–88], chemical reaction[89,90], and so on. Also, some have been utilized in the research field of tunable meta-holography.

Phase transitions

In recent years, chalcogenide phase change materials (PCMs) composed of alloys of GST have become popular in the optical storage of commercial DVDs and CDs due to their easy transition between the disordered amorphous state and ordered crystalline state by applying thermal, optical, or electrical stimuli. Moreover, GST has also been widely used in dynamic meta-holography and other metasurface research fields due to its advantages of a large refractive index difference between two states, high switching speed and reliable retention[74–80]. Lee et al. theoretically and experimentally proved the concept of an ITO-GST-ITO (IGI)-based meta-hologram panel[77]. After IGI was fabricated, an excimer pulse laser at an ultraviolet wavelength was used to achieve local crystallization of the GST film with a micrometer-scale pixel pitch and a 16k × 16k resolution. Notably, the fabrication of the GST hologram panel required the transfer of the CGH pattern from a Cr mask to an IGI layer, as shown in Fig. 2(a). The large refractive index difference between the amorphous and crystalline states caused a significant change in the reflection coefficient before and after crystallization of the GST. Holographic images could be reconstructed from CGH patterns consisting of local crystallization pixels. Zhang et al. demonstrated a switchable spin-orbit interaction via the combination of plasmonic metasurfaces with PCMs[78]. The designed meta-devices were based on a simple metal–insulator–metal (MIM) configuration in which the insulator layer consisted of GST and MgF_2 films, the bottom layer consisted of a gold ground plane, and the top array consisted of subwavelength plasmonic gold antennas. Three reflective meta-devices were fabricated and measured as a proof of concept that enabled the spin Hall effect, vortex beam generation and a hologram in the amorphous state of GST ("ON" state) separately, which disappeared in the crystalline state of GST ("OFF" state), as shown in Fig. 2(b). Zhou et al. proposed a similar approach to achieve transmissive dynamic meta-holographic encryption based on a structure in which a GST film is sandwiched between a bottom SiO_2 substrate and top gold split-ring resonator (SRR) arrays[76]. The resonance behaviors of the fixed SRR structure were completely different between the two states of GST, resulting in varying phase and amplitude modulation. The holographic reconstruction based on continuous phase modulation in the amorphous state of GST was converted to a binary phase in the crystalline state, as shown in Fig. 2(c).

Another attractive candidate material for tunable meta-holography is VO_2. This strongly correlated material exhibits an insulator-to-metal transition (IMT) under thermal, electrical, or optical stimuli[91]. The relatively low transformation temperature (approximately 340 K, 67 °C) and large refractive index contrast of VO_2 from monoclinic (insulating phase) to tetragonal (metallic phase) make it suitable for the realization of switchable metasurface device design. Driscoll et al. demonstrated the first VO_2-based tunable metasurface device, which achieved dynamic tuning of an infrared hybrid-metasurface resonance in 2008[81]. VO_2 was also used to realize switchable meta-holographic elements. Liu et al. proposed a thermally dependent dynamic meta-holography design using a vanadium dioxide integrated metasurface[83]. The unit cell was a gold split ring with VO_2 filling in the gap, as shown in the illustration of Fig. 2(d). The reconstructed images transformed from "H" to "G" as the temperature increased from 25 °C to 100 °C. Furthermore, a new approach for dynamic meta-holography at optical frequencies by utilizing a cavity incorporating an active VO_2 layer was proposed by Haimov et al.[84]. A Bragg

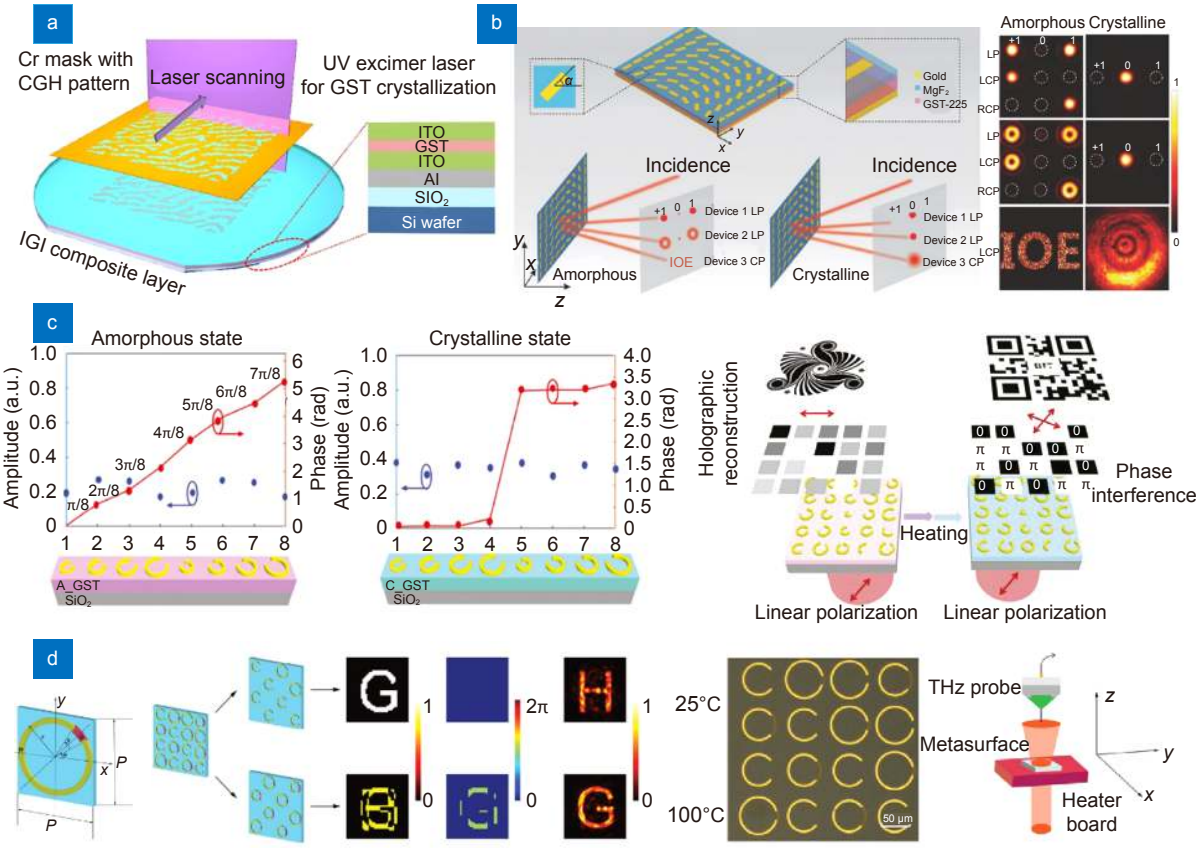

Fig. 2 | Tunable metasurface holography based on phase transitions. (**a**) Schematic of the proposed multilayered GST-based sample and its hologram recording process. A thin film of a PCM encapsulated by dielectric layers can be used for the hologram panel by means of excimer laser lithography. (**b**) Schematic of the demonstrated switchable photonic SOIs. Different optical performances of the three designed metadevices can be switched between when the GST layer is in the amorphous or crystalline state. (**c**) Schematic of double functionalities using the simultaneous phase modulation and interference strategy. The continuous phase modulation under the amorphous state can be converted to a binary phase modulation under the crystalline state. (**d**) Schematic of thermally dependent dynamic meta-holography using a vanadium dioxide integrated metasurface. The meta-hologram consists of two sets of resonators, which generate certain holographic images with predesigned amplitude and phase distributions. Figure reproduced with permission from: (a) ref.[77], (c) ref.[76], under a Creative Commons Attribution 4.0 International License; (b) ref.[78], under the terms of the Creative Commons Attribution License; (d) ref.[83], John Wiley and Sons.

reflector was introduced at the bottom, and a nearly π phase shift could be obtained from the reflected waves before and after the IMT.

Chemical reaction

Some specialized chemical reactions were also used in the dynamic control of meta-holography. For example, magnesium (Mg) has great plasmonic properties in the visible range and undergoes a phase transition from a metal to a dielectric by forming magnesium hydride (MgH_2) upon hydrogen loading[92]. By using oxygen, the phase transition is reversible through dehydrogenation.

Li et al. created dynamic meta-hologram devices consisting of plasmonic Mg nanorods that constituted addressable pixels by hydrogenation/dehydrogenation for optical information encryption design[90]. Li et al. proposed three different nanorods to demonstrate the capability for optical information processing and encryption. Gold (Au) nanorods (marked as P_2 in ref.[90] and Fig. 3(a)) were stable and irrelevant to chemical reactions. A titanium (Ti) spacer and a palladium (Pd) catalytic layer were capped on Mg nanorods to facilitate hydrogenation and dehydrogenation processes (Mg/Pd, marked as P_1 in ref.[90]), while a chromium (Cr) capping layer effectively slowed down both the hydrogenation and dehydrogenation rates of the third kind of nanorod (Mg/Pd/Cr, marked as P_3 in ref.[90]). The three kinds of different nanorods were placed in each unit cell and coded to generate different holographic images to realize information encryption and dynamic control, as shown in Fig. 3(a).

Furthermore, Li et al., in another research group, theoretically demonstrated a concept to realize an

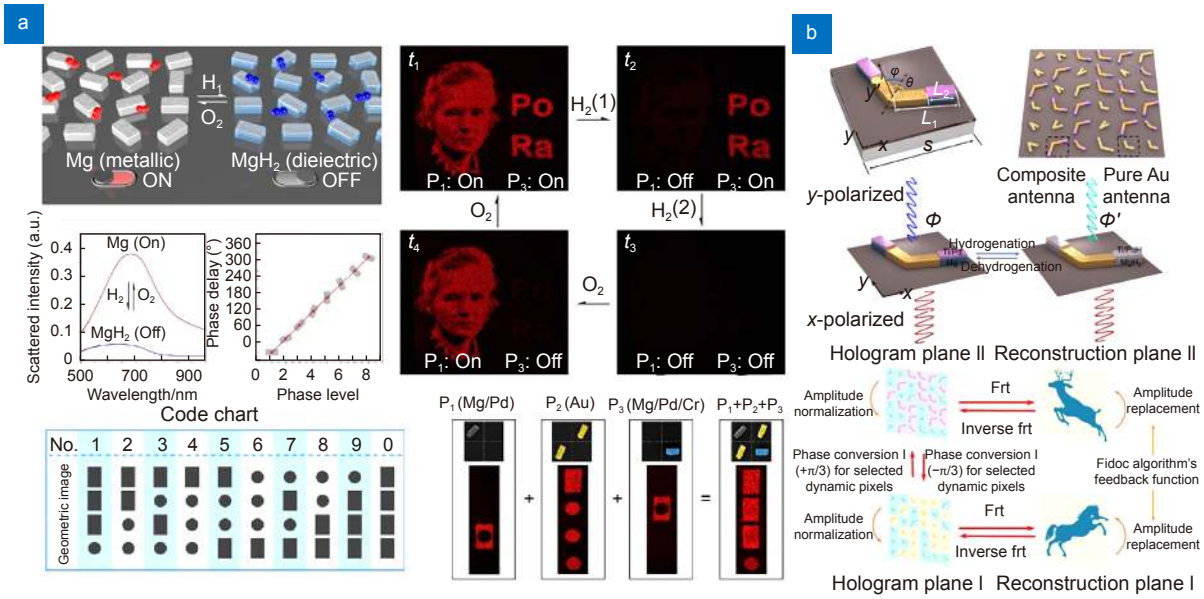

Fig. 3 | Tunable metasurface holography based on chemical reactions. (**a**) Chemically active metasurfaces allow independent manipulation of addressable subwavelength pixels at visible frequencies. Plasmonic nanorods tailored to exhibit hierarchical reaction kinetics upon hydrogenation/dehydrogenation constitute addressable pixels in multiplexed metasurfaces. (**b**) An iterative hologram algorithm based on the Fidoc method builds up a quantified phase relation, which allows the reconfigurable phase profile to reshape the reconstructed image. Figure reproduced from: (a) ref.[90], AAAS; (b) ref.[89], Optical Society of America.

addressable dynamic meta-hologram by utilizing similar hydrogenation/dehydrogenation of Mg[89]. The proposed meta-hologram devices were composed of pure Au V-shaped antennas (PVAs) and composite Mg-Au V-shaped antennas (CVAs). The scattering phase of the CVAs was uniformly shifted by π/3 before and after hydrogenation. To establish a quantified phase relation and calculate the distribution of PVAs and CVAs, an iterative hologram algorithm based on the Fidoc method was developed by the authors.

The chemical reaction method can only make a few reconstructed holographic images switchable. The speeds of hydrogenation/dehydrogenation used in these designs were too slow to achieve smooth holographic display. Chemical control methods are more suitable for achieving platforms promising for relatively simple dynamic functionalities that require no quick response, such as optical encryption and smart sensors.

Rewritable meta-holography and stretchable substrate meta-holography

In addition to the methods introduced above, there have also been some other particular and inspiring means to achieve tunable meta-holography.

As a two-dimensional material with good electronic and optical properties, graphene is a good choice to be incorporated with metasurfaces to realize tunability. Li et al. demonstrated write-once holograms for wide-angle and full-color three-dimensional images enabled by reduced graphene oxide, as shown in Fig. 4(a)[71]. They discovered that the fs laser intensity of the focal spot was correlated with the refractive index modulation in the reduced graphene oxide. The athermal photoreduction could be confined to a diffraction-limited region since the fs laser pulse removes undesired accumulative heating. Moreover, by precise control of the laser irradiance, reversible reduction and oxidation of graphene oxides could be obtained to achieve updatable reduced graphene oxide holograms.

Another interesting tunable meta-holography research work was realized by Malek et al. in 2017[87]. The authors demonstrated a reconfigurable meta-hologram with gold nanorods on a stretchable polydimethylsiloxane substrate. Stretchable metasurfaces have also been used in studies of actively tunable structural color[85,86] and zoom metalenses[88]. Stretching the substrate could change the spectrum response of the metasurface[85,86], focal length of the metalens[88], and distance of the image display plane from the meta-hologram panel[87]. By coding several reconstructed images at different distances into one piece of metasurface on a stretchable substrate, the displayed holographic images on the same observation plane can be switched by stretching the metasurface device, as shown in Fig. 4(b).

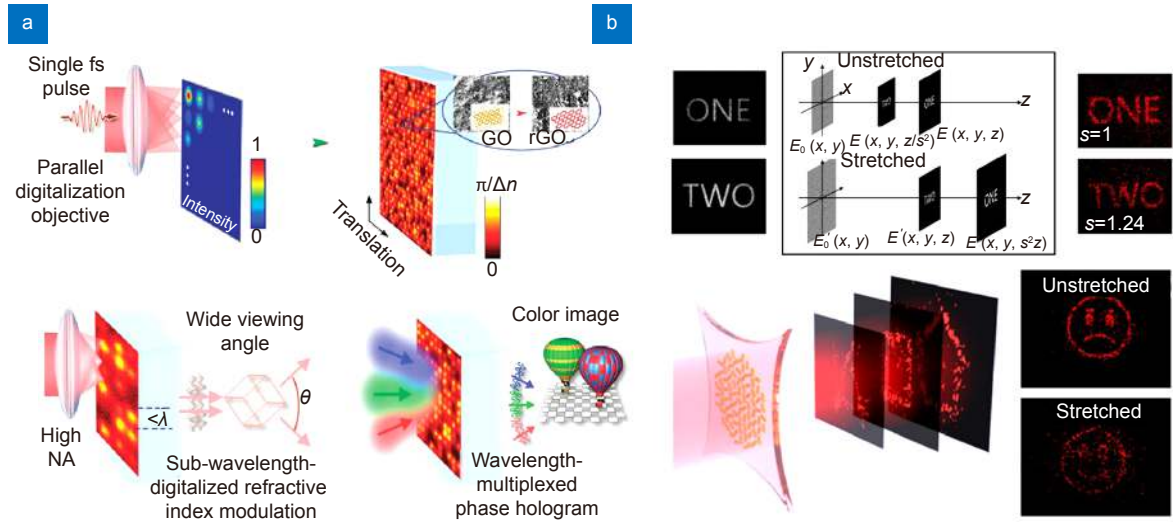

Fig. 4 | Rewritable and stretchable meta-holography methods. (**a**) Tunable metasurface hologram composed of functional graphene oxide materials for achieving 3D holography with wide viewing angles, which is rewritable by pumping with femtosecond laser pulses. (**b**) Reconfigurable phase-only computer-generated metasurface holograms with up to three image planes operating in the visible regime fabricated with gold nanorods on a stretchable polydimethylsiloxane substrate. Upon stretching, the holographic image displayed by these devices can be switched between multiple distinct images. Figure reproduced with permission from: (a) ref.[71], under a Creative Commons Attribution 4.0 International License. (b) ref.[87], American Chemical Society.

Multiplexed meta-holography

Many fundamental properties of light act as independent dimensions, such as the propagation direction, wavelength (frequency), polarization, and OAM, which enables multiplexing technologies. Multiplexing technologies have been widely used in the research fields of optical communications and optical computing to extremely extend the bandwidths or enormously increase the speed. Additionally, studies on meta-holograms can utilize similar multiplexing technologies to achieve dynamic display.

Wavelength multiplexed meta-holography

Traditional optical holography is usually displayed under a single wavelength laser, resulting from the limitation of interference principles. To achieve a colorful holographic display under white light, a rainbow hologram was invented in 1968 by Dr. Stephen A. Benton, who recorded interference patterns using a slit to eliminate vertical parallax and reduce spectral blur in the viewing output image. Furthermore, the concept of rainbow illumination was also introduced into volumetric imaging based on digital dynamic holographic devices (e.g., SLMs) to extend the viewing zone in both the vertical and longitudinal directions[93] but not for the purpose of colorful display. As diffractive elements, these digital dynamic CGH devices possess wavelength-dependent properties that make them not simple to use in reconstructed color imagery. Some special approaches (e.g., frequency filtering[94] and phase shift[95]) have been developed to realize full-color holographic display using digital dynamic CGH devices with multiwavelength illumination.

The broadband display is of great importance to the practical holographic applications. There are quite a few excellent research works to achieve broadband meta-holograms[96–98]. To achieve a colorful meta-holographic display, the abundant degrees of freedom in designing subwavelength structures[99–101] and metasurface elements[102–104] have brought about many novel approaches. In 2015, Huang et al. reported a phase-modulated multicolor meta-hologram element that consisted of a two-dimensional array of pixels[99], as shown in Fig 5(a). There were four subpixels (two for blue, one for red and one for green) in each pixel. The subpixel had a 4×4 aluminum nanorod pattern. The nanorods in each subpixel representing different colors possessed different reflection spectra due to the various geometrical sizes. The method proposed in this research work was a good idea to set up a corresponding relationship between the geometrical parameters of subwavelength structures and response spectra while not bringing additional fabrication difficulties. However, the orientation directions of all nanorods were the same, and this limitation made the device only obtain a phase difference of 0–π. Wang et al. proposed a full phase-controlled multiwavelength

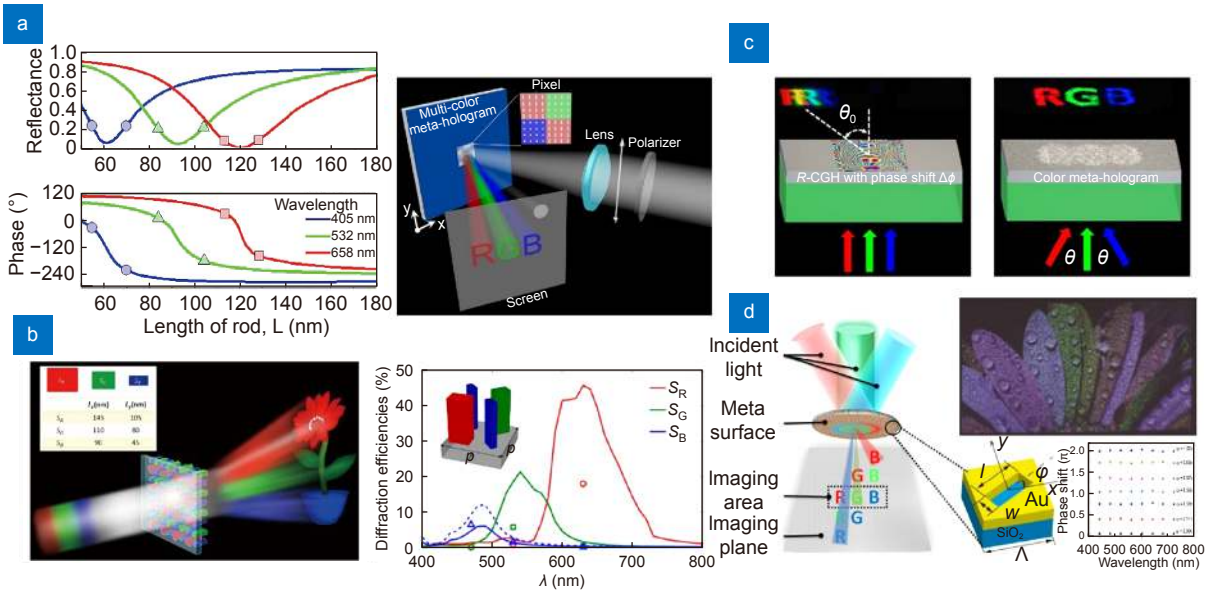

Fig. 5 | Wavelength-multiplexed meta-holography. (**a**) Schematic of the designed multicolor meta-hologram under linearly polarized illumination. The phase-modulated multicolor meta-hologram enables the formation of polarization-dependent images in three primary colors. (**b**) Schematic of visible-frequency silicon metasurfaces formed by three kinds of nanoblocks multiplexed in a subwavelength unit, which are capable of wavefront manipulation for red, green, and blue light simultaneously. (**c**) Schematic of full-color plasmonic metasurface holograms with both amplitude and phase modulations for reconstructing 2D and 3D holographic color images. (**d**) Schematic of the off-axis illumination method for the full-color meta-hologram. The image on the top right shows the experimental results of a colorful flower image based on plasmonic nanoslit antennas. Figure reproduced with permission from: (a) ref.[99], (b) ref.[100], (c) ref.[103], American Chemical Society. (d) ref.[102], under a Creative Commons Attribution NonCommercial License 4.0.

meta-hologram based on a similar approach[100] (Fig. 5(b)). The response spectra were also modulated by the length and width of the nanoblocks, while the phase delay was generated by the orientation angles of the nanoblocks. The increased degree of freedom in rotation of the nanoblocks made it possible to achieve any desired phase delay. In addition to the various subwavelength structures, other properties of the metasurface have also been used to realize wavelength-multiplexed meta-holograms. Generally, similar to other diffractive elements, the sizes and diffraction angles of reconstructed holographic images are also related to the working wavelengths for normal meta-hologram elements. In 2016, Wan et al. reported a wavelength-multiplexed full-color meta-hologram design based on phase-shift methods[103], as shown in Fig. 5(c). The additional phase shift $\Delta\varphi = -k_\lambda \sin(\theta_\lambda)\Delta x$ along the x-axis was encoded into the metasurface and corresponded to the tilted angle of incident light with wavelength λ. This approach does not require complicated geometrical parameters or special materials of nanostructures to eliminate the color dispersion and is suitable for many-wavelength-multiplexed meta-hologram design. Li et al. demonstrated a seven-wavelength meta-hologram and achieved a 1.39 times larger color gamut than the traditional red/green/blue design (see Fig. 5(d)). Furthermore, Zhang et al. combined a similar off-axis illumination method and polarization-dependent geometric phase to achieve a colorful meta-hologram in both transmission and reflection spaces for the first time[104].

Notably, most colorful meta-holography research works were focused not on achieving dynamic display but on full color display, data storage and information encryption. However, the reconstructed images could be switched by changing the wavelengths of the incident light, so these research works conform to the definition of dynamic meta-holograms.

Polarization multiplexed meta-holography

As a transverse wave, light possesses a polarization property that specifies the orientation of the oscillation, namely, the direction of the electric field. Traditional CGH devices are polarization-insensitive (e.g., diffractive optical elements and freeform optics) or can only work at specific polarization states (e.g., liquid crystal SLMs). Meta-hologram elements consisting of anisotropic subwavelength structures can offer the capability to respond variously according to the polarization state of the

interacting light. This characteristic makes them appropriate for polarization-multiplexed holography. In 2013, Montelongo and Chen et al., from two independent research groups, proposed and theoretically and experimentally demonstrated the concept of polarization-multiplexed meta-holograms separately[105,106]. The two independent images for each polarization were coded into independent diffraction patterns, and the two patterns were merged to obtain one metasurface element. The reconstructed images could be switched by changing the polarization state of incident light from one direction to the other orthogonal direction (from 0° to 90°). The merged metasurface produced the two images simultaneously with half the intensity at 45°. Although the results from the two groups were similar, Montelongo et al. designed metasurface elements by the amplitude modulation method, while Chen et al. implemented a four phase level design to achieve this purpose. All these basic research works provided the possibility of achieving switchable meta-holographic display by changing the polarization state of incident light.

Besides linear polarization states, spin angular momentum (circular polarization states) also can be regarded as a fundamental degree of freedom to encode the meta-holography[107–109]. In 2015, Wen et al. experimentally demonstrated a helicity-multiplexed meta-hologram with two symmetrically distributed off-axis images that were interchangeable by switching the helicity of the incident light beam[110]. Arbabi et al. demonstrated metasurface devices with complete control of the polarization and phase, including polarization-switchable phase holograms[111]. Compared with Chen's work based on four phase levels in 2013, Arbabi's design could realize arbitrary phase distributions for two orthogonal polarization states by anisotropic dielectric metasurfaces. The input ($\boldsymbol{E}^{\mathrm{in}}$) and output waves ($\boldsymbol{E}^{\mathrm{out}}$) at each pixel could be related by a general Jones matrix,

$$\boldsymbol{T}=\begin{bmatrix} T_{xx} & T_{xy} \\ T_{yx} & T_{yy} \end{bmatrix},$$

as $\boldsymbol{E}^{\mathrm{out}}=\boldsymbol{T}\boldsymbol{E}^{\mathrm{in}}$. In this way, any desired polarization and phase control can be achieved by implementing any unitary and symmetric Jones matrix at each pixel. Furthermore, Mueller et al. developed and advanced the method and combined the geometric phase and propagation phase to achieve two independent and arbitrary phase distributions for any pair of orthogonal polarization states (linear, elliptical or circular)[112]. Mueller et al. demonstrated this method by two independent reconstructed images for left-hand and right-hand circular polarization states separately, as shown in Fig. 6(a). In

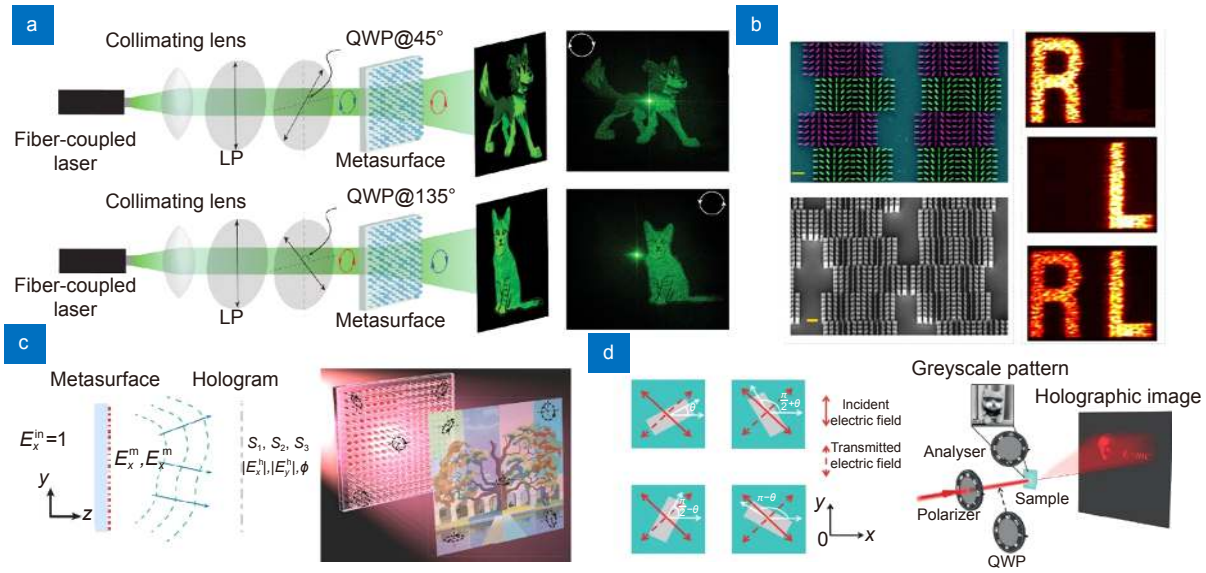

Fig. 6 | Polarization-multiplexed meta-holography. (**a**) Schematic diagram and experimental realization of a cartoon dog and cat with tailored Si nanofins for orthogonal circular polarization multiplexing. (**b**) Chiral holograms that project different images depending on the handedness of the reference beam by incorporating a geometric phase. (**c**) Schematic of a structurally birefringent dielectric metasurface projecting a desired polarization pattern encoding an RGB image with arbitrary complexity. (**d**) Schematic of Malus metasurfaces based on a one-to-four mapping and two independent information channels for intensity and phase manipulation. Figure reproduced with permission from: (a) ref.[112], American Physical Society. (b) ref.[113], under a Creative Commons Attribution NonCommercial License 4.0. (c) ref.[115], American Chemical Society. (d) ref.[116], under a Creative Commons Attribution 4.0 International License.

addition, the geometric phase method can also be incorporated with other phase modulation approaches. In 2016, Khorasaninejad et al. achieved broadband and chiral binary meta-holograms by revisiting and implementing the principle of the detour phase and geometric phase[113]. Similarly, two switchable independent images could be achieved for left-hand and right-hand circular polarization states separately, as shown in Fig. 6(b). This device also demonstrated the advantages of broadband operation (from the visible to the near-infrared) and high efficiency (as high as 75%). These methods utilizing the propagation phase, detour phase and geometric phase provided more degrees of freedom for metasurface polarization optics.

However, most research on polarization-dependent meta-holograms has focused on two orthogonal states. In 2018, Zhao et al. integrated twelve polarization manipulation channels for various phase profiles into a single birefringent vectorial meta-hologram[114]. In 2019, by using structurally birefringent dielectric metasurfaces, Arbabi et al. proposed and demonstrated vectorial holograms with arbitrary polarization states in which the color information was converted to Stokes parameters to be stored and reconstructed as a monochromatic hologram image[115]. To realize the reconstructed image, as shown in Fig. 6(c), a modified Gerchberg-Saxton algorithm was developed. To code 8-bit (0−255) color images, the Stokes parameters S_i were coded as $S_i=(X-128)/128$, where i represents 1, 2, or 3 and X represents the value for the R, G, or B channel.

The success of the advances in metasurfaces researches in recent years, to a great extent, should be attributed to the development of classical optical theories, e.g., the generalized Snell's law. Currently, the developments still continuously provide us with interesting and instructive ideas. For example, Deng et al. noted the orientation degeneracy implied in Malus's law and found a one-to-M mapping between the light irradiance and Pancharatnam–Berry phase, which could be applied to design advanced geometric metasurfaces. They proposed a Malus-metasurface-assisted polarization multiplexing method and generated a near-field grayscale pattern as well as an independent far-field holographic image simultaneously with one sample, as shown in Fig. 6(d)[116].

These polarization-multiplexed meta-hologram works implemented many modulation approaches and implied potential applications in dual-channel display, anti-counterfeiting, encryption, security and data storage.

Angle multiplexed meta-holography

The angular response characteristics are significant for diffractive optics, including gratings, diffractive optical elements, and metasurfaces. The corresponding input and output angles are correlated by physical optics theories, which make each pair of them an independent channel. This optical property provides a new degree of freedom to achieve multiplexed meta-holography.

In 2017, Kamali et al. introduced an angle-multiplexed metasurface design composed of dielectric U-shaped units with reflective high contrast in which linear momentum depending on the incident angle was added to display different images at different tilted angles of incidence[117]. The geometrical sizes of the U-shapes in different dimensions were optimized to achieve a full 2π phase shift. The structure provided independent phase control under a TE-polarized light beam at 0° and 30° incident angles. Two different images were coded as different phase profiles of the metasurface corresponding to different angles, so the designed angle-multiplexed meta-hologram element created two independent projected images under 0° and 30° separately, as shown in Fig. 7(a). In this way, Kamali et al. created two independent channels corresponding to different incident angles to display two images. In 2020, Wang et al. proposed an angle-multiplexed multichannel metasurface to achieve arbitrary spatially varying light fields[118]. The designed angle-multiplexed metasurfaces had the capability to independently control the handedness and azimuth and possessed four channels, as shown in Fig. 7(b). The proposed methods enable realization of full Poincaré beams, dual-way switching and vectorial print images, and optical information communication. Furthermore, the number of channels could be expanded by combining angle multiplexing methods with other multiplexing methods. As we discussed above in section wavelength multiplexed meta-holography, an additional phase shift along a selected axis could be encoded into the metasurface to achieve wavelength-multiplexed meta-holography[102–104]. To correct the phase shift for different wavelengths and display the reconstructed images at desired positions, the incident light beams should possess the right tilted angles corresponding to the wavelengths. Therefore, the reconstructed images could be switched by changing the wavelengths of incident light beams or incident angles. Strictly speaking, these research works utilized wavelength multiplexing methods and angle multiplexing methods simultaneously.

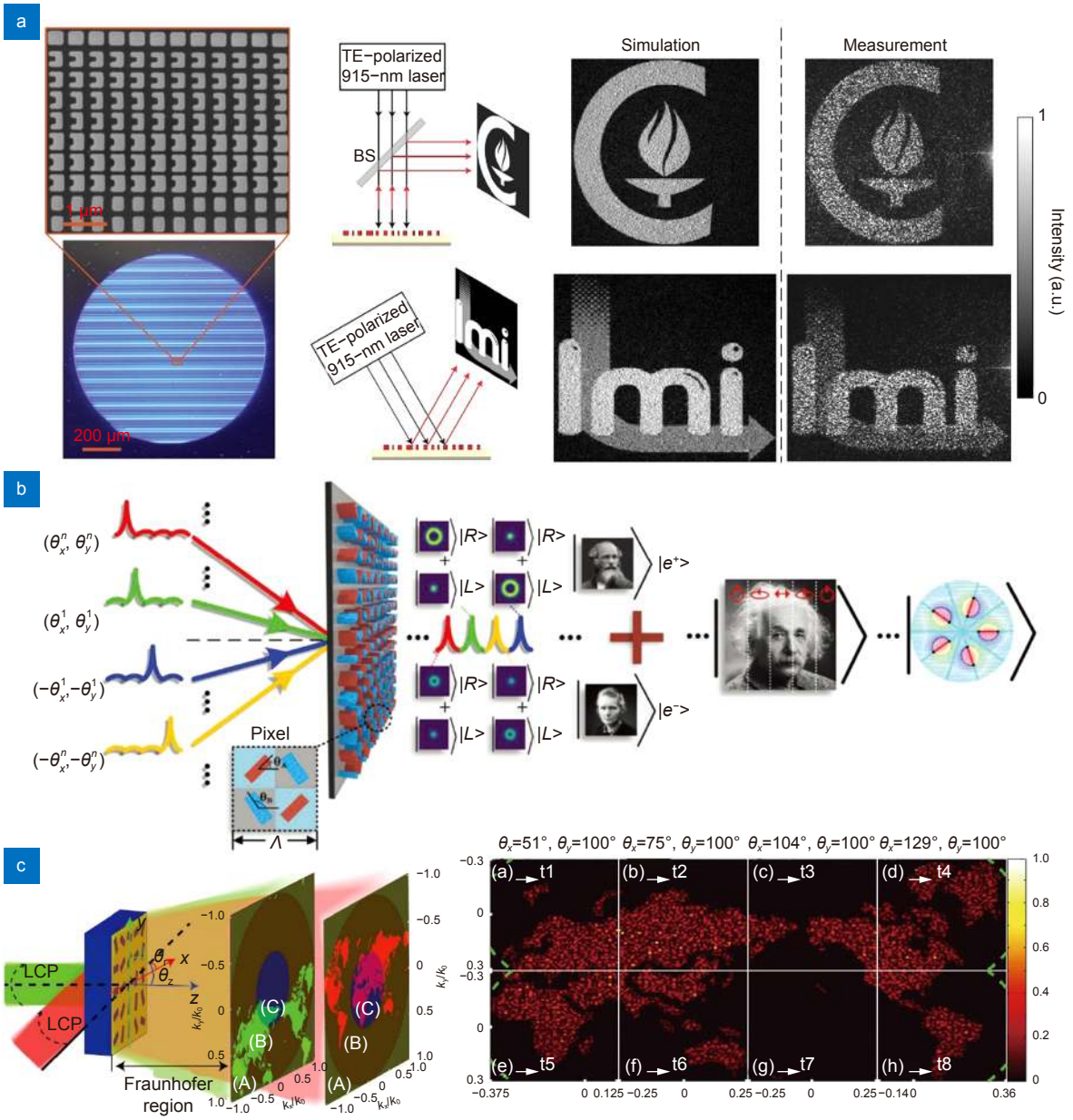

Fig. 7 | Angle-multiplexed meta-holography. (**a**) Angle-multiplexed metasurfaces composed of reflective high-contrast dielectric U-shaped meta-atoms, whose response under illumination from different angles can be controlled independently. (**b**) Schematic illustrations of the coherent pixel polarization meta-holography scheme and angle-multiplexed metasurface. (**c**) Schematic illustrations of the imaging information capacity increment by transferring the evanescent wave to the propagating wave through off-axis illumination. Figure reproduced with permission from: (a) ref.[117], under a Creative Commons Attribution 4.0 International License; (b) ref.[118], John Wiley and Sons; (c) ref.[119], Royal Society of Chemistry.

In addition to achieving a multichannel meta-hologram, other types of dynamic meta-holograms can also be realized by angle multiplexing methods. In 2017, Zhang et al. proposed an ultrahigh-capacity meta-hologram design by encoding information in nanohole arrays[119]. The imaging information capacity could be increased 11.5 times compared with the usual metasurface element, and the compressed image information could be reconstructed by changing the tilted incident angle, as shown in Fig. 7(c). The high capacity of the designed metasurface was achieved by transferring the evanescent wave to the propagating wave. At normal incidence, much imaging information could not be reconstructed in the far field since it was hidden in the evanescent wave region. However, hidden information could be exhibited via off-axis illumination. The reconstructed meta-holographic image appeared like a dynamically varying scroll painting when changing the incident angle of the light

beam. This method could also be used in large capacity optical storage and lithography technologies.

OAM multiplexed meta-holography

As a fundamental property of photons, the orbital angular momentum (OAM) plays a significant role in many applications of light, including optical communication, stimulated emission depletion microscopy, and optical tweezers, due to the special helical wavefront, doughnut-shaped intensity distribution and unbounded set of orthogonal helical modes (named topological charge *l*). Additionally, recently, many approaches have been proposed to achieve dynamic meta-holograms by considering OAM as a degree of freedom.

Ren et al. proposed OAM-multiplexed meta-holography designs for the first time in 2019 and achieved dynamic holographic display, as shown in Fig. 8(a)[120]. In this paper, Ren et al. demonstrated a design of a 10-bit OAM-multiplexed meta-hologram that could achieve 2^{10} different OAM-dependent holographic images. In addition to the multiplexed design, two other kinds of metasurface OAM holograms, including OAM-conserving and OAM-selective meta-holograms, were also demonstrated theoretically and experimentally. Fang et al. demonstrated similar OAM-preserved, OAM-selective and OAM-multiplexed holograms based on the SLM platform and proved the potential applications of OAM holography for high-security encryption[121]. The research work from Ren et al. in 2019[120] was based on pure phase modulations of metasurfaces and suffered from the challenge of channel crosstalk, which limited the number of channels. Therefore, Ren et al. developed and optimized the method, proposed complex-amplitude metasurface-based OAM holography and demonstrated it with 200

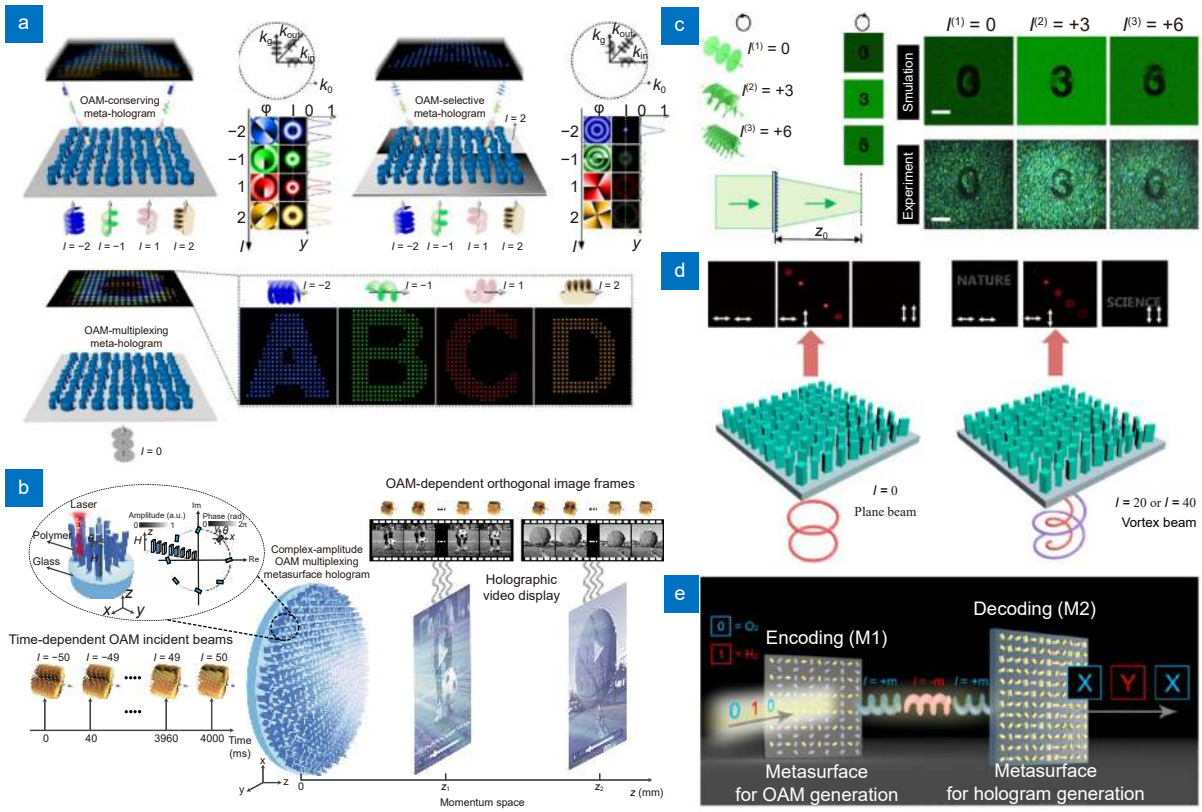

Fig. 8 | OAM-multiplexed meta-holography. (**a**) Schematic of metasurface orbital angular momentum holography by utilizing the strong orbital angular momentum selectivity offered by meta-holograms consisting of GaN nanopillars with discrete spatial frequency distributions. (**b**) Schematic of ultrahigh-dimensional OAM-multiplexed holography based on a large-scale complex-amplitude OAM-multiplexed metasurface hologram. (**c**) Schematic of the OAM meta-transformer designed based on three OAM states, which can reconstruct "0", "3" and "6". (**d**) Schematic of OAM multiplexing in different polarization channels using a birefringent metasurface for holographic encryption. (**e**) Schematic of a dynamic metasurface for holographic pattern switching through OAM multiplexing. Switchable vector beams of different polarization states and switchable vortex beams of different topological charges can be implemented through simple hydrogenation and dehydrogenation of the same metasurfaces. Figure reproduced with permission from: (a) ref.[120], (c) ref.[123], (e) ref.[125], under a Creative Commons Attribution 4.0 International license; (b) ref.[122] , Springer Nature; (d) ref.[124], under an ACS AuthorChoice License.

independent OAM channels, as shown in Fig. 8(b)[122]. The out-of-plane height of the nanopillar offered amplitude control, while its in-plane rotation generated the phase response. A 3D metasurface sample was fabricated by a femtosecond laser, which provided possibilities for large-area fabrication. Moreover, the demonstrated reconstructed images were shown as two independent smooth holographic videos at two different planes, which suggested the capability for realizing 3D holography.

There were also other approaches to achieve OAM-multiplexed meta-holography. In 2019, Jin et al. proposed a dielectric multimomentum meta-transformer design that could reconstruct different OAM beams with different topological charges into distinct on-axis images, as shown in Fig. 8(c)[123]. The meta-transformer possessed fixed phase profiles itself but could synergize the intrinsic properties (e.g., OAM and linear momentum) of light to achieve a dynamic meta-hologram. The total phase profile of the transmitted beam was $\psi_{\mathrm{T}}(x_0, y_0) = \psi_{\mathrm{OAM}}(x_0, y_0) + \psi_{\mathrm{meta}}(x_0, y_0)$, where $\psi_{\mathrm{meta}}(x_0, y_0)$ was fixed after fabrication and defined by the orientation of the nanostructure array and $\psi_{\mathrm{OAM}}(x_0, y_0)$ was the phase profile of incident OAM beams, which was changeable by switching the topological charge l. Vivid "R", "G" and "B" reconstructed patterns were demonstrated under red, green, and blue illumination separately to prove the possibilities in color holographic display applications.

The OAM-multiplexed meta-hologram methods could also be combined with other modulation methods to achieve richer dynamic modulation functions. For example, in 2020, Zhou et al. proposed a holographic encryption design based on OAM-multiplexed meta-holograms in different polarization channels[124]. In this way, the selective holographic image could only be reconstructed under the exact light beam with the right topological charge and a specific polarization state, as shown in Fig. 8(d). Another interesting research work was reported by Yu et al. in 2019[125]. In section Chemical reaction, we introduced the dynamic meta-hologram that could be achieved by chemical reactions of Mg due to its phase transition property between a metal and a dielectric. In 2019, Yu et al. proposed a dynamic meta-holography design based on two metasurface elements. The first metasurface was composed of Mg nanorods, which could generate switchable vortex beams with different topological charges (l=m and l=$-m$) by hydrogenation and dehydrogenation reactions. The second metasurface could generate different reconstructed images in response to the OAM beams with designed topological charges m and $-m$. By using these two cascaded metasurfaces, a dynamic meta-hologram was achieved, as shown in Fig. 8(e).

Space channel multiplexed meta-holography

One can obtain some inspiration for designing dynamic meta-holograms by comparing dynamic meta-holograms and common 2D display technologies in daily life. There are several approaches to achieve good 2D display apart from pixel display screens. One practical approach is the cinematographic method, which projects different images from a continuous video at different times; the other way is dividing whole images into many subgraphs and displaying them in different combinations at different times, e.g., the digital tube of an electronic scoreboard.

In 2020, Izumi et al. demonstrated a meta-holographic movie by the cinematographic approach[126]. Forty-eight meta-hologram channels were arrayed on a substrate, and the substrate was fixed on a two-axis electric moving stage and moved in a designed sequence at a designed speed. Each hologram channel was sequentially illuminated and each holographic frame was reconstructed on a screen, as shown in Fig. 9(a). A smooth movie could be achieved with a frame rate of 30 frames per second. In the same year, Gao et al. proposed dynamic 3D meta-hologram designs with large frame number and high frame rate based on space channel methods[127]. The meta-hologram samples were divided into many space channels and illuminated by a high-speed coded structured light beam. In addition to a cinematographic meta-holographic video with twenty frames, a space channel multiplexed meta-hologram of 28 bits was also demonstrated, which could display 2^{28} different frames, as shown in Fig. 9(b). To generate a high precision coded structured light beam, a dynamic space beam coding module consisting of a DMD, a tube lens and an objective lens was built, which made the high frame rate of the meta-hologram system achieve 9523 frames per second.

Nonlinear wavelength multiplexed meta-holography

Most research works on metasurfaces were operated in the linear optics regime, including meta-holography. However, researchers have extended metasurface research to the nonlinear optics regime in recent years[128–130]. For example, in 2015, Li et al. were inspired by the concept of spin-rotation coupling, experimentally demonstrated nonlinear metasurfaces containing

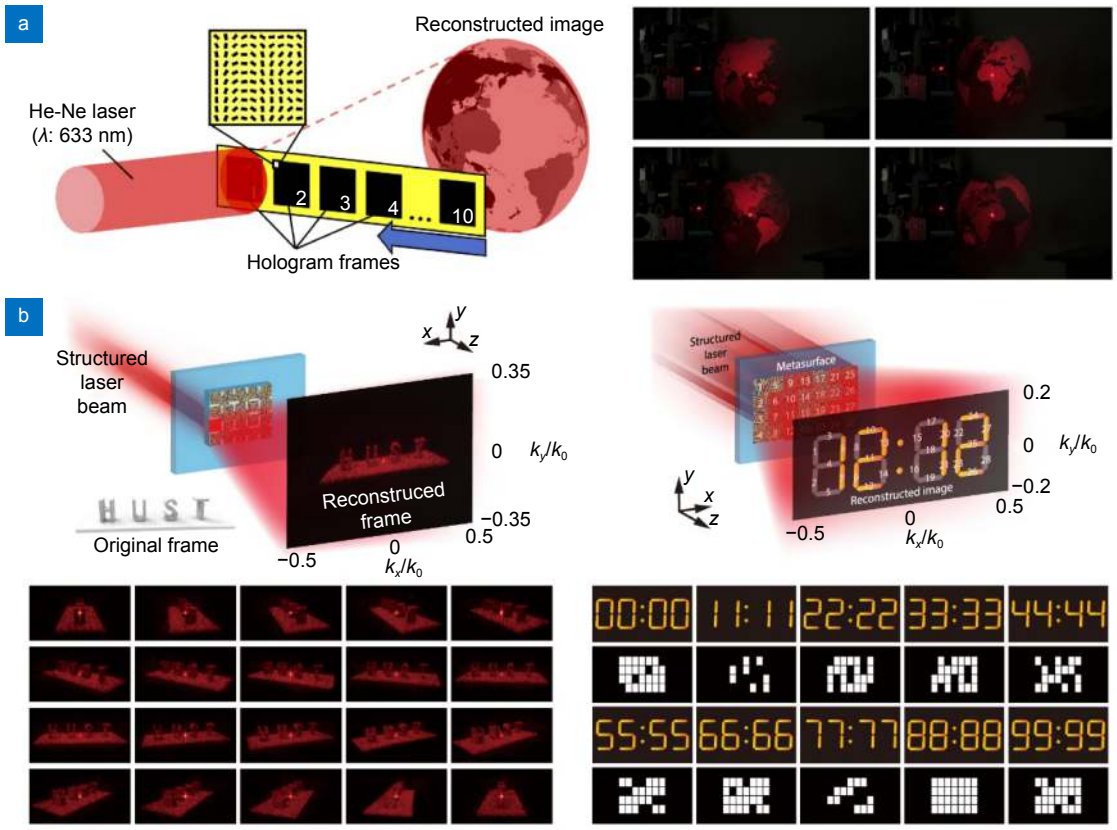

Fig. 9 | Space channel-multiplexed meta-holography. (**a**) Schematic of a cinematography-inspired metasurface holographic movie. Time-lapse images were reconstructed using sequentially arranged metasurface hologram frames. (**b**) Schematic of a space channel multiplexed metasurface. A structured laser beam opens a specific space channel in the designed sequence, and continuous frames of a holographic video are displayed. Figure reproduced with permission from: (a) ref.[126], under the terms of the OSA Open Access Publishing Agreement. (b) ref.[127], under a Creative Commons Attribution License 4.0.

plasmonic antennas and theoretically proved that the concept could be applied to dielectric and bulk-like metamaterials[128].

In 2016, Ye et al. combined nonlinear metasurfaces and several multiplexing methods to achieve spin- and wavelength-multiplexed nonlinear meta-holography[131]. Since these metasurfaces are still static elements, nonlinear meta-holography could also be regarded as a special multiplexing method. The split-ring resonator was selected as the meta-atom to design the nonlinear metasurface due to its strong polarization properties in linear optics and high efficiency of second-harmonic generation. The reported design allowed the construction of multiple independent holographic images by fundamental and second harmonic waves with different spins separately, as shown in Fig. 10(a). Nonlinear meta-holography provides independent and crosstalk-free channels for holographic reconstruction, which is suitable for multichannel holographic display, optical data storage and optical encryption.

Incident light field multiplexed meta-holography

The coded information for holographic reconstruction of all the research works we discussed above was fabricated on the metasurface elements and not embedded in the incident light beams. Even for methods with modulation of incident light, e.g., OAM multiplexing methods[120,122,123], the OAM beam with a specific topological charge was only used to select and open the target channel and did not contain any information for holographic reconstruction.

In 2020, Qu et al. proposed an interesting research work about incident light field-multiplexed meta-holography (named the "reprogrammable meta-hologram" in ref.[132]), which divided the hologram information into two matrices[132]. One information matrix was coded into the metasurface as usual; however, the other matrix was coded into the incident light beam. The phase matrix of incident light was an additional degree of freedom to design the meta-hologram. This work paved a new way to optical information encryption. In this way, the

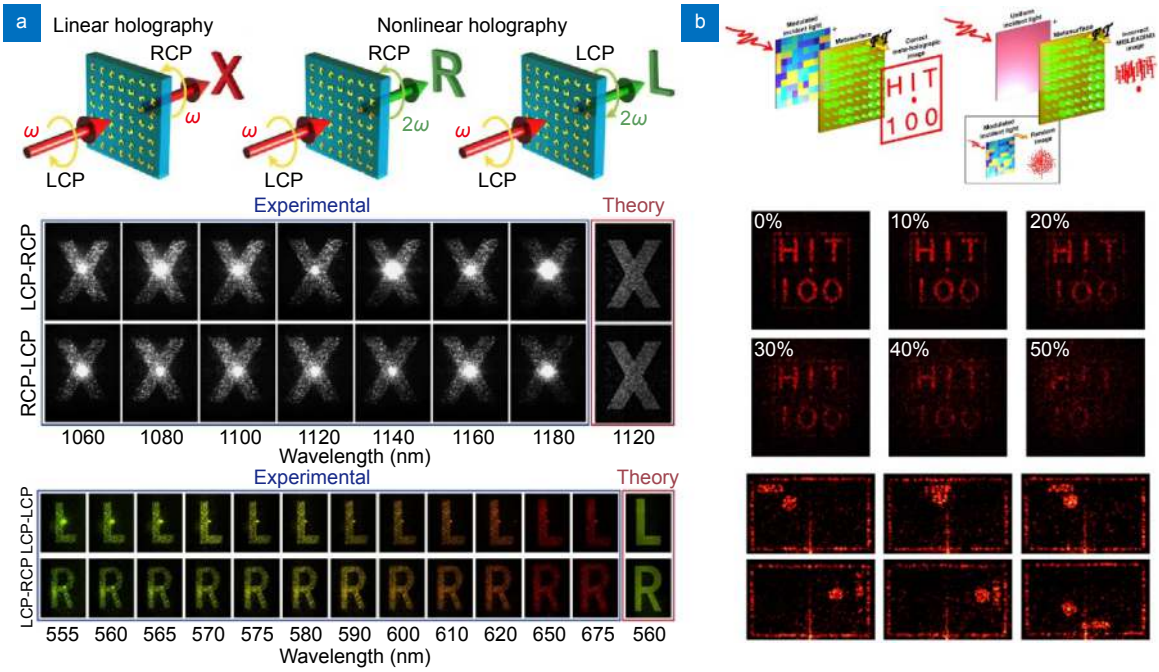

Fig. 10 | Nonlinear and reprogrammable meta-holography. (**a**) Nonlinear holographic metasurfaces. Linear holography for reconstruction of the letter "X" at infrared wavelengths, and nonlinear holographic images for reconstruction of the letters encoded in different circular polarization states. (**b**) Schematic of a reprogrammable metasurface with arbitrary holographic images for optical encryption. Holographic image of the metasurface when it is illuminated with the modulated incident beam and an incorrect uniform laser beam. By playing a set of holographic frames sequentially, a video of the pinball game from start to end can be achieved. Figure reproduced with permisson from: (a) ref.[131], (b) ref.[132], under a Creative Commons Attribution 4.0 International License.

method could achieve infinite arbitrary holographic images and videos by a static metasurface and dynamic incident light, as shown in Fig. 10(b).

Multi-dimensions multiplexed meta-holography

In practical applications, to increase frame numbers and degrees of freedom to encode holograms, multiple methods can be utilized to design a meta-hologram element simultaneously. As we discussed above, Li et al. demonstrated a colorful meta-hologram by making use of wavelength and angle multiplexed method at same time. And Yu et al. proposed a dynamic meta-holography design based on two metasurface elements, in which first element was achieved by chemical reaction method and second one utilized OAM multiplexed approach. Moreover, in 2018, Jin et al. demonstrated (2^6–1) spin- and wavelength-encoded holograms by manipulating six bases of incident photons simultaneously to reconstruct 6-bit wavelength- and spin-dependent multicolor images as shown in Fig. 11(a)[133]. Furthermore, in 2020, Deng et al. proposed a multi-freedom metasurface, which combined geometric Pancharatnam–Berry phase and detour phase. The method allowed us to control the complex amplitude and polarization of the wavefront simultaneously with totally decoupled wavelength and incident angle dependence, and ultimately to achieve full-color complex-amplitude vectorial meta-hologram as shown in Fig. 11(b)[134].

Besides dynamic holographic display, there were also some interesting research works about combining meta-hologram and other imaging methods recently. In 2020, Li et al. experimentally demonstrated a three-channel metasurface which can simultaneously record a continuous grayscale nanoprinting image in the near field and project two independent holographic images in the far field[135]. In the same year, Dai et al. proposed a "three-in-one" metasurface device which simultaneously acted as a structural-color nanoprint element, a polarization-controlled grayscale metasurface image displayer and a phase-modulated meta-hologram[136]. These excellent works inspired researchers to explore more possibilities of meta-holograms.

Discussion and outlook

In summary, we have discussed recent advances in dynamic meta-holography. Compared with traditional CGH devices, metasurfaces have many advantages for holographic display, such as a large FOV, a high

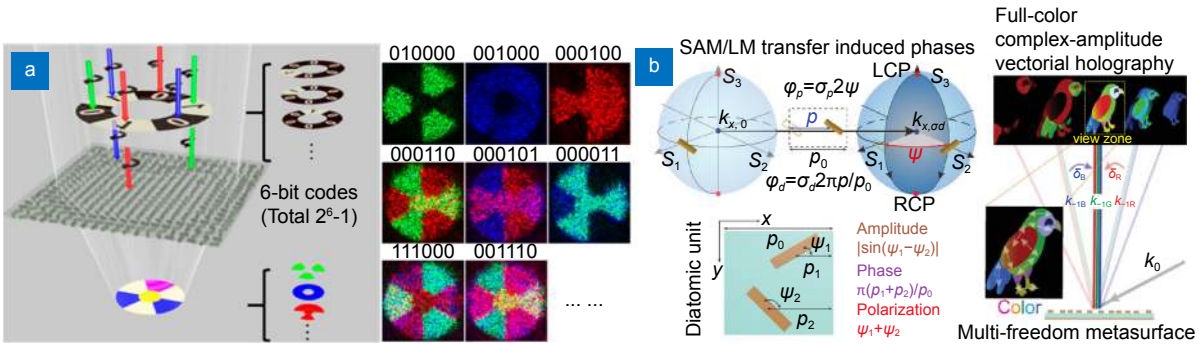

Fig. 11 | Multi-dimensions multiplexed meta-holography. (**a**) Schematic of (2^6–1) spin- and wavelength-encoded holograms by manipulating six bases of incident photons simultaneously to reconstructed 6-bit wavelength- and spin-dependent multicolor images. (**b**) Schematic of a multi-freedom metasurface which achieving full-color complex-amplitude vectorial meta-hologram by combining geometric Pancharatnam-Berry phase and detour phase. Figure reproduced with permission from: (a) ref.[133], American Chemical Society; (b) ref.[134], John Wiley and Sons.

resolution, and low noise. Benefiting from the powerful capabilities in modulating the amplitude, phase, and polarization of light, metasurfaces provide multiple degrees of freedom for dynamic hologram design. In this paper, we reviewed typical research works on dynamic meta-holography based on various methods, including tunable metasurfaces, multiplexed metasurfaces and multi-dimensions multiplexed metasurfaces. From the discussion above, it can be found that dynamic meta-holography has many applications in optical storage, anti-counterfeiting, security, lithography, optical encryption and holographic display.

For smooth holographic display, it is essentially required to achieve infinite numbers of vivid frames at a considerable frame rate. In this respect, some progress has been made through multiple methods. However, these methods are still far from achieving the ultimate holographic display, as shown in science-fiction films. One ideal and general approach to achieve a dynamic meta-hologram is to control the interaction between waves and each nanostructure of the metasurface at high speed, similar to the display strategy of LED pixel arrays or LCD screen in showing 2D images in our daily life. In other words, we need a metasurface-based SLM with good performance in terms of the refresh rate, modulation efficiency and broadband response in the visible range.

Recently, several groups reported their research progress in electrically tunable metasurface-based SLMs[68,72,137]. Although these works were based on different materials and methods, all of these designs were one-dimensional (1D) metasurface-based SLMs. 1D SLMs are suitable for the applications of beam steering, 1D focusing and lidar but not for holographic display. 2D metasurface-based SLMs in the visible range are still challenging and difficult to achieve due to the limitations of fabrication technologies. Therefore, OAM[122], space channel[127] and reprogrammable[132] methods provide promising and alternative approaches to achieve dynamic meta-holography in specific application scenarios due to their excellent performance in terms of frame number and frame rate. With the rapid development of nanofabrication technologies and creative design methods, we believe that ideal dynamic meta-holography will appear in the near future.

References

1. Matharu AS, Jeeva S, Ramanujam PS. Liquid crystals for holographic optical data storage. *Chem Soc Rev* **36**, 1868–1880 (2007).
2. Hvilsted S, Sánchez C, Alcalá R. The volume holographic optical storage potential in azobenzene containing polymers. *J Mater Chem* **19**, 6641–6648 (2009).
3. Chen LF, Zhao DM. Optical color image encryption by wavelength multiplexing and lensless Fresnel transform holograms. *Opt Express* **14**, 8552–8560 (2006).
4. Rivenson Y, Zhang YB, Günaydın H, Teng D, Ozcan A. Phase recovery and holographic image reconstruction using deep learning in neural networks. *Light Sci Appl* **7**, 17141 (2018).
5. Leach J, Sinclair G, Jordan P, Courtial J, Padgett MJ et al. 3D manipulation of particles into crystal structures using holographic optical tweezers. *Opt Express* **12**, 220–226 (2004).
6. Curtis JE, Koss BA, Grier DG. Dynamic holographic optical tweezers. *Opt Commun* **207**, 169–175 (2002).
7. Gabor D. A new microscopic principle. *Nature* **161**, 777–778 (1948).
8. Brown BR, Lohmann AW. Complex spatial filtering with binary masks. *Appl Opt* **5**, 967–969 (1966).
9. Mok F, Diep J, Liu HK, Psaltis D. Real-time computer-generated hologram by means of liquid-crystal television spatial light modulator. *Opt Lett* **11**, 748–750 (1986).
10. Hahn J, Kim H, Lim Y, Park G, Lee B. Wide viewing angle

dynamic holographic stereogram with a curved array of spatial light modulators. *Opt Express* **16**, 12372–12386 (2008).
11. Huang LL, Zhang S, Zentgraf T. Metasurface holography: from fundamentals to applications. *Nanophotonics* **7**, 1169–1190 (2018).
12. Zhao RZ, Huang LL, Wang YT. Recent advances in multi-dimensional metasurfaces holographic technologies. *PhotoniX* **1**, 20 (2020).
13. Ma XL, Pu MB, Li X, Guo YH, Luo XG. All-metallic wide-angle metasurfaces for multifunctional polarization manipulation. *Opto-Electron Adv* **2**, 180023 (2019).
14. Guo JY, Wang T, Quan BG, Zhao H, Gu CZ et al. Polarization multiplexing for double images display. *Opto-Electron Adv* **2**, 180029 (2019).
15. Zhang YB, Liu H, Cheng H, Tian JG, Chen SQ. Multidimensional manipulation of wave fields based on artificial microstructures. *Opto-Electron Adv* **3**, 200002 (2020).
16. Cai T, Wang GM, Zhang XF, Liang JG, Zhuang YQ et al. Ultrathin polarization beam splitter using 2-D Transmissive phase gradient Metasurface. *IEEE Trans Antennas Propag* **63**, 5629–5636 (2015).
17. Khorasaninejad M, Zhu W, Crozier KB. Efficient polarization beam splitter pixels based on a dielectric metasurface. *Optica* **2**, 376–382 (2015).
18. Zhao ZY, Pu MB, Gao H, Jin JJ, Li X et al. Multispectral optical metasurfaces enabled by achromatic phase transition. *Sci Rep* **5**, 15781 (2015).
19. Gao H, Pu MB, Li X, Ma XL, Zhao ZY et al. Super-resolution imaging with a Bessel lens realized by a geometric metasurface. *Opt Express* **25**, 13933–13943 (2017).
20. Khorasaninejad M, Chen WT, Devlin RC, Oh J, Zhu AY et al. Metalenses at visible wavelengths: Diffraction-limited focusing and subwavelength resolution imaging. *Science* **352**, 1190–1194 (2016).
21. Khorasaninejad M, Capasso F. Metalenses: versatile multifunctional photonic components. *Science* **358**, eaam8100 (2017).
22. Shrestha S, Overvig AC, Lu M, Stein A, Yu NF. Broadband achromatic dielectric metalenses. *Light Sci Appl* **7**, 85 (2018).
23. Wang SM, Wu PC, Su VC, Lai YC, Chen MK et al. A broadband achromatic metalens in the visible. *Nat Nanotechnol* **13**, 227–232 (2018).
24. Dou KH, Xie X, Pu MB, Li X, Ma XL et al. Off-axis multi-wavelength dispersion controlling metalens for multi-color imaging. *Opto-Electron Adv* **3**, 190005 (2020).
25. Pu MB, Li X, Ma XL, Wang YQ, Zhao ZY et al. Catenary optics for achromatic generation of perfect optical angular momentum. *Sci Adv* **1**, e1500396 (2015).
26. Gao H, Li Y, Chen LW, Jin JJ, Pu MB et al. Quasi-Talbot effect of orbital angular momentum beams for generation of optical vortex arrays by multiplexing metasurface design. *Nanoscale* **10**, 666–671 (2018).
27. Jin JJ, Luo J, Zhang XH, Gao H, Li X et al. Generation and detection of orbital angular momentum via metasurface. *Sci Rep* **6**, 24286 (2016).
28. Yang KP, Pu MB, Li X, Ma XL, Luo J et al. Wavelength-selective orbital angular momentum generation based on a plasmonic metasurface. *Nanoscale* **8**, 12267–12271 (2016).
29. Karimi E, Schulz SA, De Leon I, Qassim H, Upham J et al. Generating optical orbital angular momentum at visible wavelengths using a plasmonic metasurface. *Light Sci Appl* **3**, e167 (2014).
30. Li GX, Kang M, Chen SM, Zhang S, Pun EYB et al. Spin-enabled Plasmonic Metasurfaces for manipulating orbital angular momentum of light. *Nano Lett* **13**, 4148–4151 (2013).
31. Zhu XL, Yan W, Levy U, Mortensen NA, Kristensen A. Resonant laser printing of structural colors on high-index dielectric metasurfaces. *Sci Adv* **3**, e1602487 (2017).
32. Sun S, Zhou ZX, Zhang C, Gao YS, Duan ZH et al. All-dielectric full-color printing with TiO_2 Metasurfaces. *ACS Nano* **11**, 4445–4452 (2017).
33. Huo PC, Song MW, Zhu WQ, Zhang C, Chen L et al. Photorealistic full-color nanopainting enabled by a low-loss metasurface. *Optica* **7**, 1171–1172 (2020).
34. Cheng F, Gao J, Luk TS, Yang XD. Structural color printing based on plasmonic metasurfaces of perfect light absorption. *Sci Rep* **5**, 11045 (2015).
35. Proust J, Bedu F, Gallas B, Ozerov I, Bonod N. All-dielectric colored Metasurfaces with silicon mie resonators. *ACS Nano* **10**, 7761–7767 (2016).
36. Lee GY, Sung J, Lee B. Recent advances in metasurface hologram technologies (Invited paper). *ETRI J* **41**, 10–22 (2019).
37. Zheng GX, Mühlenbernd H, Kenney M, Li GX, Zentgraf T et al. Metasurface holograms reaching 80% efficiency. *Nat Nanotechnol* **10**, 308–312 (2015).
38. Huang LL, Chen XZ, Mühlenbernd H, Zhang H, Chen SM et al. Three-dimensional optical holography using a plasmonic metasurface. *Nat Commun* **4**, 2808 (2013).
39. Wang L, Kruk S, Tang HZ, Li T, Kravchenko I et al. Grayscale transparent metasurface holograms. *Optica* **3**, 1504–1505 (2016).
40. Zhang XH, Jin JJ, Wang YQ, Pu MB, Li X et al. Metasurface-based broadband hologram with high tolerance to fabrication errors. *Sci Rep* **6**, 19856 (2016).
41. Devlin RC, Khorasaninejad M, Chen WT, Oh J, Capasso F. Broadband high-efficiency dielectric metasurfaces for the visible spectrum. *Proc Natl Acad Sci USA* **113**, 10473–10478 (2016).
42. Huang K, Liu H, Garcia-Vidal FJ, Hong MH, Luk'yanchuk B et al. Ultrahigh-capacity non-periodic photon sieves operating in visible light. *Nat Commun* **6**, 7059 (2015).
43. Butt H, Montelongo Y, Butler T, Rajesekharan R, Dai Q et al. Carbon nanotube based high resolution holograms. *Adv Mater* **24**, OP331–OP336 (2012).
44. Walther B, Helgert C, Rockstuhl C, Setzpfandt F, Eilenberger F et al. Photonics: spatial and spectral light shaping with Metamaterials (Adv. Mater. 47/2012). *Adv Mater* **24**, 6251 (2012).
45. Ni XJ, Kildishev AV, Shalaev VM. Metasurface holograms for visible light. *Nat Commun* **4**, 2807 (2013).
46. Wang Q, Zhang XQ, Xu YH, Gu JQ, Li YF et al. Broadband metasurface holograms: toward complete phase and amplitude engineering. *Sci Rep* **6**, 32867 (2016).
47. Chong KE, Wang L, Staude I, James AR, Dominguez J et al.

Efficient polarization-insensitive complex Wavefront control using Huygens' Metasurfaces based on dielectric resonant meta-atoms. *ACS Photonics* **3**, 514–519 (2016).
48. Overvig AC, Shrestha S, Malek SC, Lu M, Stein A et al. Dielectric metasurfaces for complete and independent control of the optical amplitude and phase. *Light Sci Appl* **8**, 92 (2019).
49. Jiang Q, Jin GF, Cao LC. When metasurface meets hologram: principle and advances. *Adv Opt Photonics* **11**, 518–576 (2019).
50. Chen SQ, Liu WW, Li ZC, Cheng H, Tian JG. Metasurface-empowered optical multiplexing and multifunction. *Adv Mater* **32**, 1805912 (2020).
51. Li ZL, Yu SH, Zheng GX. Advances in exploiting the degrees of freedom in nanostructured metasurface design: from 1 to 3 to more. *Nanophotonics* **9**, 3699–3731 (2020).
52. Cui T, Bai BF, Sun HB. Tunable Metasurfaces based on active materials. *Adv Funct Mater* **29**, 1806692 (2019).
53. Nemati A, Wang Q, Hong MH, Teng JH. Tunable and reconfigurable metasurfaces and metadevices. *Opto-Electron Adv* **1**, 180009 (2018).
54. Horie Y, Arbabi A, Arbabi E, Kamali SM, Faraon A. High-speed, phase-dominant spatial light modulation with silicon-based active resonant antennas. *ACS Photonics* **5**, 1711–1717 (2018).
55. Sun J, Timurdogan E, Yaacobi A, Hosseini ES, Watts MR. Large-scale nanophotonic phased array. *Nature* **493**, 195–199 (2013).
56. Rahmani M, Xu L, Miroshnichenko AE, Komar A, Camacho-Morales R et al. Reversible thermal tuning of all-dielectric Metasurfaces. *Adv Funct Mater* **27**, 1700580 (2017).
57. Lewi T, Evans HA, Butakov NA, Schuller JA. Ultrawide thermo-optic tuning of PbTe meta-atoms. *Nano Lett* **17**, 3940–3945 (2017).
58. Gu JQ, Singh R, Liu XJ, Zhang XQ, Ma YF et al. Active control of electromagnetically induced transparency analogue in terahertz metamaterials. *Nat Commun* **3**, 1151 (2012).
59. Makarov S, Kudryashov S, Mukhin I, Mozharov A, Milichko V et al. Tuning of magnetic optical response in a dielectric nanoparticle by ultrafast Photoexcitation of dense electron –hole plasma. *Nano Lett* **15**, 6187–6192 (2015).
60. Lewi T, Iyer PP, Butakov NA, Mikhailovsky AA, Schuller JA. Widely tunable infrared antennas using free carrier refraction. *Nano Lett* **15**, 8188–8193 (2015).
61. Chen HT, Padilla WJ, Zide JMO, Gossard AC, Taylor AJ et al. Active terahertz metamaterial devices. *Nature* **444**, 597–600 (2006).
62. Watts CM, Shrekenhamer D, Montoya J, Lipworth G, Hunt J et al. Terahertz compressive imaging with metamaterial spatial light modulators. *Nat Photonics* **8**, 605–609 (2014).
63. Chen HT, Padilla WJ, Cich MJ, Azad AK, Averitt RD et al. A metamaterial solid-state terahertz phase modulator. *Nat Photonics* **3**, 148–151 (2009).
64. Iyer PP, Pendharkar M, Schuller JA. Electrically reconfigurable Metasurfaces using Heterojunction resonators. *Adv Opt Mater* **4**, 1582–1588 (2016).
65. Huang YW, Lee HWH, Sokhoyan R, Pala RA, Thyagarajan K et al. Gate-tunable conducting oxide Metasurfaces. *Nano Lett* **16**, 5319–5325 (2016).
66. Chen YB, Ke F, Ci PH, Ko C, Park T et al. Pressurizing field-effect transistors of few-layer MoS_2 in a diamond anvil cell. *Nano Lett* **17**, 194–199 (2017).
67. Thyagarajan K, Sokhoyan R, Zornberg L, Atwater HA. Millivolt modulation of Plasmonic Metasurface optical response via ionic conductance. *Adv Mater* **29**, 1701044 (2017).
68. Shirmanesh GK, Sokhoyan R, Wu PC, Atwater HA. Electro-optically tunable multifunctional Metasurfaces. *ACS Nano* **14**, 6912–6920 (2020).
69. Lee S, Baek S, Kim TT, Cho H, Lee S et al. Metamaterials for enhanced optical responses and their application to active control of terahertz waves. *Adv Mater* **32**, 2000250 (2020).
70. Liu PQ, Luxmoore IJ, Mikhailov SA, Savostianova NA, Valmorra F et al. Highly tunable hybrid metamaterials employing split-ring resonators strongly coupled to graphene surface plasmons. *Nat Commun* **6**, 8969 (2015).
71. Li XP, Ren HR, Chen X, Liu J, Li Q et al. Athermally photoreduced graphene oxides for three-dimensional holographic images. *Nat Commun* **6**, 6984 (2015).
72. Li SQ, Xu XW, Veetil RM, Valuckas V, Paniagua-Domínguez R et al. Phase-only transmissive spatial light modulator based on tunable dielectric metasurface. *Science* **364**, 1087–1090 (2019).
73. Komar A, Paniagua-Domínguez R, Miroshnichenko A, Yu YF, Kivshar YS et al. Dynamic beam switching by liquid crystal tunable dielectric Metasurfaces. *ACS Photonics* **5**, 1742–1748 (2018).
74. de Galarreta CR, Alexeev AM, Au YY, Lopez-Garcia M, Klemm M et al. Nonvolatile reconfigurable phase-change Metadevices for beam steering in the near infrared. *Adv Funct Mater* **28**, 1704993 (2018).
75. Yin XH, Steinle T, Huang LL, Taubner T, Wuttig M et al. Beam switching and bifocal zoom lensing using active plasmonic metasurfaces. *Light Sci Appl* **6**, e17016 (2017).
76. Zhou HQ, Wang YT, Li XW, Wang Q, Wei QS et al. Switchable active phase modulation and holography encryption based on hybrid metasurfaces. *Nanophotonics* **9**, 905–912 (2020).
77. Lee SY, Kim YH, Cho SM, Kim GH, Kim TY et al. Holographic image generation with a thin-film resonance caused by chalcogenide phase-change material. *Sci Rep* **7**, 41152 (2017).
78. Zhang M, Pu MB, Zhang F, Guo YH, He Q et al. Plasmonic metasurfaces for switchable photonic spin –orbit interactions based on phase change materials. *Adv Sci* **5**, 1800835 (2018).
79. Raeis-Hosseini N, Rho J. Metasurfaces Based on phase-change material as a reconfigurable platform for multifunctional devices. *Materials* **10**, 1046 (2017).
80. Qu YR, Li Q, Du KK, Cai L, Lu J et al. Dynamic thermal emission control based on ultrathin plasmonic metamaterials including phase-changing material GST. *Laser Photonics Rev* **11**, 1700091 (2017).
81. Driscoll T, Palit S, Qazilbash MM, Brehm M, Keilmann F et al. Dynamic tuning of an infrared hybrid-metamaterial resonance using vanadium dioxide. *Appl Phys Lett* **93**, 024101 (2008).
82. Goldflam MD, Liu MK, Chapler BC, Stinson HT, Sternbach AJ et al. Voltage switching of a VO_2 memory metasurface using

ionic gel. *Appl Phys Lett* **105**, 041117 (2014).
83. Liu XB, Wang Q, Zhang XQ, Li H, Xu Q et al. Thermally dependent dynamic meta-holography using a vanadium dioxide integrated Metasurface. *Adv Opt Mater* **7**, 1900175 (2019).
84. Haimov T, Aydin K, Scheuer J. Reconfigurable holograms using VO_2-based tunable metasurface. *IEEE J Sel Top Quantum Electron* **27**, 4700308 (2021).
85. Song SC, Ma XL, Pu MB, Li X, Liu KP et al. Actively tunable structural color rendering with tensile substrate. *Adv Opt Mater* **5**, 1600829 (2017).
86. Zhang C, Jing JX, Wu YK, Fan YB, Yang WH et al. Stretchable all-dielectric Metasurfaces with polarization-insensitive and full-spectrum response. *ACS Nano* **14**, 1418–1426 (2020).
87. Malek SC, Ee HS, Agarwal R. Strain multiplexed Metasurface holograms on a stretchable substrate. *Nano Lett* **17**, 3641–3645 (2017).
88. Ee HS, Agarwal R. Tunable Metasurface and flat optical zoom lens on a stretchable substrate. *Nano Lett* **16**, 2818–2823 (2016).
89. Li TY, Wei QS, Reineke B, Walter F, Wang YT et al. Reconfigurable metasurface hologram by utilizing addressable dynamic pixels. *Opt Express* **27**, 21153–21162 (2019).
90. Li JX, Kamin S, Zheng GX, Neubrech F, Zhang S et al. Addressable metasurfaces for dynamic holography and optical information encryption. *Sci Adv* **4**, eaar6768 (2018).
91. Zylbersztejn A, Mott NF. Metal-insulator transition in vanadium dioxide. *Phys Rev B* **11**, 4383–4395 (1975).
92. Duan XY, Kamin S, Sterl F, Giessen H, Liu N. Hydrogen-regulated chiral Nanoplasmonics. *Nano Lett* **16**, 1462–1466 (2016).
93. Kozacki T, Chlipala M, Choo HG. Fourier rainbow holography. *Opt Express* **26**, 25086–25097 (2018).
94. Lin SF, Kim ES. Single SLM full-color holographic 3-D display based on sampling and selective frequency-filtering methods. *Opt Express* **25**, 11389–11404 (2017).
95. Jesacher A, Bernet S, Ritsch-Marte M. Colour hologram projection with an SLM by exploiting its full phase modulation range. *Opt Express* **22**, 20530–20541 (2014).
96. Wang DP, Hwang Y, Dai YM, Si GY, Wei SB et al. Broadband high-efficiency chiral splitters and holograms from dielectric Nanoarc Metasurfaces. *Small* **15**, 1900483 (2019).
97. Xie ZW, Lei T, Si GY, Wang XY, Lin J et al. Meta-holograms with full parameter control of Wavefront over a 1000 nm Bandwidth. *ACS Photonics* **4**, 2158–2164 (2017).
98. Huang K, Liu H, Si GY, Wang Q, Lin J et al. Photon-nanosieve for ultrabroadband and large-angle-of-view holograms. *Laser Photonics Rev* **11**, 1700025 (2017).
99. Huang YW, Chen WT, Tsai WY, Wu PC, Wang CM et al. Aluminum Plasmonic multicolor meta-hologram. *Nano Lett* **15**, 3122–3127 (2015).
100. Wang B, Dong FL, Li QT, Yang D, Sun CW et al. Visible-frequency dielectric Metasurfaces for Multiwavelength achromatic and highly dispersive holograms. *Nano Lett* **16**, 5235–5240 (2016).
101. Zhao WY, Liu BY, Jiang H, Song J, Pei YB et al. Full-color hologram using spatial multiplexing of dielectric metasurface. *Opt Lett* **41**, 147–150 (2016).
102. Li X, Chen LW, Li Y, Zhang XH, Pu MB et al. Multicolor 3D meta-holography by broadband plasmonic modulation. *Sci Adv* **2**, e1601102 (2016).
103. Wan WW, Gao J, Yang XD. Full-color Plasmonic Metasurface holograms. *ACS Nano* **10**, 10671–10680 (2016).
104. Zhang XH, Pu MB, Guo YH, Jin JJ, Li X et al. Colorful Metahologram with independently controlled images in transmission and reflection spaces. *Adv Funct Mater* **29**, 1809145 (2019).
105. Montelongo Y, Tenorio-Pearl JO, Milne WI, Wilkinson TD. Polarization switchable diffraction based on subwavelength plasmonic nanoantennas. *Nano Lett* **14**, 294–298 (2014).
106. Chen WT, Yang KY, Wang CM, Huang YW, Sun G et al. High-efficiency broadband meta-hologram with polarization-controlled dual images. *Nano Lett* **14**, 225–230 (2014).
107. Zhang F, Pu MB, Li X, Gao P, Ma XL et al. All-dielectric Metasurfaces for simultaneous giant circular asymmetric transmission and Wavefront shaping based on asymmetric photonic spin–orbit interactions. *Adv Funct Mater* **27**, 1704295 (2017).
108. Deng ZL, Deng JH, Zhuang X, Wang S, Li KF et al. Diatomic Metasurface for Vectorial holography. *Nano Lett* **18**, 2885–2892 (2018).
109. Wang Q, Plum E, Yang QL, Zhang XQ, Xu Q et al. Reflective chiral meta-holography: multiplexing holograms for circularly polarized waves. *Light Sci Appl* **7**, 25 (2018).
110. Wen DD, Yue FY, Li GX, Zheng GX, Chan K et al. Helicity multiplexed broadband metasurface holograms. *Nat Commun* **6**, 8241 (2015).
111. Arbabi A, Horie Y, Bagheri M, Faraon A. Dielectric metasurfaces for complete control of phase and polarization with subwavelength spatial resolution and high transmission. *Nat Nanotechnol* **10**, 937–943 (2015).
112. Balthasar Mueller JP, Rubin NA, Devlin RC, Groever B, Capasso F. Metasurface Polarization optics: independent phase control of arbitrary orthogonal states of polarization. *Phys Rev Lett* **118**, 113901 (2017).
113. Khorasaninejad M, Ambrosio A, Kanhaiya P, Capasso F. Broadband and chiral binary dielectric meta-holograms. *Sci Adv* **2**, e1501258 (2016).
114. Zhao RZ, Sain B, Wei QS, Tang CC, Li XW et al. Multichannel vectorial holographic display and encryption. *Light Sci Appl* **7**, 95 (2018).
115. Arbabi E, Kamali SM, Arbabi A, Faraon A. Vectorial holograms with a dielectric metasurface: ultimate polarization pattern generation. *ACS Photonics* **6**, 2712–2718 (2019).
116. Deng LG, Deng J, Guan ZQ, Tao J, Chen Y et al. Malus-metasurface-assisted polarization multiplexing. *Light Sci Appl* **9**, 101 (2020).
117. Kamali SM, Arbabi E, Arbabi A, Horie Y, Faraji-Dana MS et al. Angle-multiplexed Metasurfaces: encoding independent wavefronts in a single metasurface under different illumination angles. *Phys Rev X* **7**, 041056 (2017).
118. Wang EL, Niu JB, Liang YH, Li HL, Hua YL et al. Complete control of multichannel, angle-multiplexed, and arbitrary spatially varying polarization fields. *Adv Opt Mater* **8**, 1901674 (2020).
119. Zhang XH, Jin JJ, Pu MB, Li X, Ma XL et al. Ultrahigh-capacity dynamic holographic displays via anisotropic nanoholes. *Nanoscale* **9**, 1409–1415 (2017).

120. Ren HR, Briere G, Fang XY, Ni PN, Sawant R et al. Metasurface orbital angular momentum holography. *Nat Commun* **10**, 2986 (2019).
121. Fang XY, Ren HR, Gu M. Orbital angular momentum holography for high-security encryption. *Nat Photonics* **14**, 102–108 (2020).
122. Ren HR, Fang XY, Jang J, Bürger J, Rho J et al. Complex-amplitude metasurface-based orbital angular momentum holography in momentum space. *Nat Nanotechnol* **15**, 948–955 (2020).
123. Jin L, Huang YW, Jin ZW, Devlin RC, Dong ZG et al. Dielectric multi-momentum meta-transformer in the visible. *Nat Commun* **10**, 4789 (2019).
124. Zhou HQ, Sain B, Wang YT, Schlickriede C, Zhao RZ et al. Polarization-encrypted orbital angular momentum multiplexed metasurface holography. *ACS Nano* **14**, 5553–5559 (2020).
125. Yu P, Li JX, Li X, Schütz G, Hirscher M et al. Generation of switchable singular beams with dynamic metasurfaces. *ACS Nano* **13**, 7100–7106 (2019).
126. Izumi R, Ikezawa S, Iwami K. Metasurface holographic movie: a cinematographic approach. *Opt Express* **28**, 23761–23770 (2020).
127. Gao H, Wang YX, Fan XH, Jiao BZ, Li TA et al. Dynamic 3D meta-holography in visible range with large frame number and high frame rate. *Sci Adv* **6**, eaba8595 (2020).
128. Li GX, Chen SM, Pholchai N, Reineke B, Wong PWH et al. Continuous control of the nonlinearity phase for harmonic generations. *Nat Mater* **14**, 607–612 (2015).
129. Segal N, Keren-Zur S, Hendler N, Ellenbogen T. Controlling light with metamaterial-based nonlinear photonic crystals. *Nat Photonics* **9**, 180–184 (2015).
130. Tymchenko M, Gomez-Diaz JS, Lee J, Nookala N, Belkin MA et al. Gradient nonlinear Pancharatnam-berry metasurfaces. *Phys Rev Lett* **115**, 207403 (2015).
131. Ye WM, Zeuner F, Li X, Reineke B, He S et al. Spin and wavelength multiplexed nonlinear metasurface holography. *Nat Commun* **7**, 11930 (2016).
132. Qu GY, Yang WH, Song QH, Liu YL, Qiu CW et al. Reprogrammable meta-hologram for optical encryption. *Nat Commun* **11**, 5484 (2020).
133. Jin L, Dong ZG, Mei ST, Yu YF, Wei Z et al. Noninterleaved Metasurface for (2^6–1) Spin- and wavelength-encoded holograms. *Nano Lett* **18**, 8016–8024 (2018).
134. Deng ZL, Jin MK, Ye X, Wang S, Shi T et al. Full-color complex-amplitude Vectorial holograms based on multi-freedom metasurfaces. *Adv Funct Mater* **30**, 1910610 (2020).
135. Li ZL, Chen C, Guan ZQ, Tao J, Chang S et al. Three-channel Metasurfaces for simultaneous meta-holography and meta-nanoprinting: a single-cell design approach. *Laser Photonics Rev* **14**, 2000032 (2020).
136. Dai Q, Guan ZQ, Chang S, Deng LG, Tao J et al. A single-celled tri-functional Metasurface enabled with triple manipulations of light. *Adv Funct Mater* **30**, 2003990 (2020).
137. Park J, Jeong BG, Kim SI, Lee D, Kim J et al. All-solid-state spatial light modulator with independent phase and amplitude control for three-dimensional LiDAR applications. *Nat Nanotechnol* **16**, 69–76 (2021).

Acknowledgements

We are grateful for financial supports from China Postdoctoral Science Foundation (2019M662597) and Open Funding of State Key Laboratory of Optical Tech- nologies for Microfabrication (2019).

Author contributions

H. Gao proposed the manuscript. X. H. Fan revised and reproduced figures. W. Xiong and M. H. Hong supervised the manuscript writing. All authors commented on the manuscript.

Competing interests

The authors declare no competing financial interests.